Robotica (2006) volume 24, pp. 355–363. © 2005 Cambridge University Press
doi:10.1017/S0263574705002274 Printed in the United Kingdom

Joint angle variations analyses of the two link planar manipulator in welding by using inverse kinematics

S. Bulut* and M. B. Terzioğlu

Cumhuriyet University, Mechanical Engineering Department, 58140, Sivas
e-mail: sbulut@cumhuriyet.edu.tr

(Received in Final Form: June 7, 2005, first published online 23 November 2005)

SUMMARY
In this paper, the joint angles of a two link planar manipulator are calculated by using inverse kinematics equations together with some geometric equalities. For a given position of the end-effector the joint angle and angular velocity of the links are derived. The analyses contains many equations which have to be solved. However, the solutions are rather cumbersome and complicated, therefore a program is written in *Fortran 90* in order to do, the whole calculation and data collection. The results are given at the end of this paper.

KEYWORDS: Two link planar manipulator; Inverse kinematics; Joint angles; Angular velocity; Forward kinematics.

I. INTRODUCTION

The forward kinematics problem always has a unique solution which can be obtained simply by evaluating the forward equations.[1] On the contrary, inverse kinematics does the reverse. In inverse kinematics, given a desired position and orientation for the end-effector of the robot a set of joint variables can be determine that achieve the desired position and orientation. Generally, an inverse kinematic problem may or may not have a solution. Also, if a solution exists it may not be a unique. Furthermore, inverse kinematic equations are complicated and nonlinear functions of the joint variables, therefore the solutions may be difficult to obtain even if they exist.[2]

In inverse kinematics, the equations are much more difficult to solve directly. Generally, it is necessary to develop efficient and systematic techniques that exploit the paticular kinematic structure of the manipulator. Although, in one way the method is very effective in finding the solution because it uses geometric approaches as well, still there is not one solution which can be apply to all robots. Therefore, for different robots different solutions are needed.

II. TWO LINK PLANAR MANIPULATOR

The manipulator is consist of two links and a end-effector which is fixed at the end of the second link, as it is shown in Fig. 1. In this figure, the end-effector is moving linearly between the points A and B.

In Fig. 1, l_1 and l_2 are the lenghts of the first and second link of the manipulator, θ_1 is the joint angle between x coordinate frame and the first link of the manipulator, θ_2 is the angle between the first and second link of the manipulator. While the end-effector is moving between A and B in a linear motion, the workspace of the manipulator will be as shown in Fig. 2.

This type of linear movement is desired, especially in welding applications in order to have a linear and homogeneous welding seam. The welding seam $[AB]$ can be divided into many steps as shown in Fig. 3. Every point coressponds to diferent links position and joint angles which may calculated by using inverse kinematics equations.[3]

III. INVERSE KINEMATIC ANALYSES

When the end-effector of the manipulator is moving from A to B in a linear motion, as it is shown in Fig. 1, the joint angles θ_1 and θ_2 change according to the manipulator links position l_1 and l_2.

Let's assume that the end-effector is doing a welding operation between A and B points, as it is shown in Fig 1. In this figure, A is the starting point, where the welding starts and B is the final point where it ends. In order to figure out the joint angles of the manipulator along $[AB]$, inverse kinematics equations are used. Finding the inverse kinematics solutions at the point A and B will not give us clear idea how the end-effector is behaving along the welding seam. Therefore it is necessary to find the inverse kinematic solution of every step points along $[AB]$. Doing this computation by hand is rather difficult, complicated and cumbersome. For this reason, a program is written in *Fortran 90* which calculates the joint angles and links position of the manipulator. The program is written based on forward and inverse kinematic equations. In order to drive inverse kinematics equations,[4] homogeneous equations are used together with some geometric equalities according to the Denavit Hartenberger (D-H) representation.

For any given starting and ending points, the program calculates the manipulators links positions, joint angles and joint angle velocities which will presented at the end of this paper. The main purpose of this program is to figure out the end effector position by calculating the variations in the first and second joint angles θ_1 and θ_2, respectively.

Let's assume that the end-effector is passing $[AB]$ in limited step points. Under this condition, x and y coordinates

* Corresponding author.

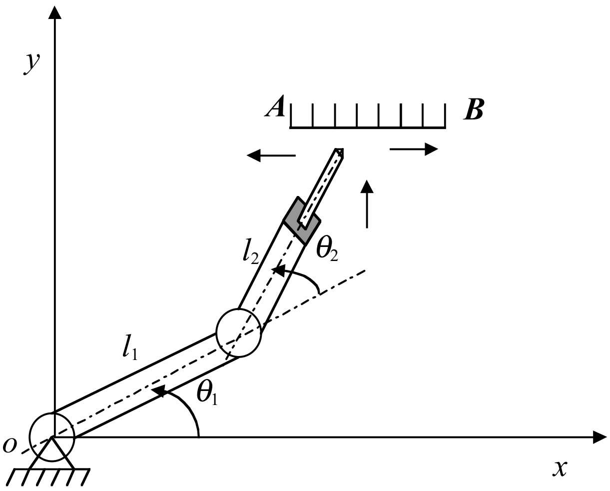

Fig. 1. Linear movement of the end effector from A to B

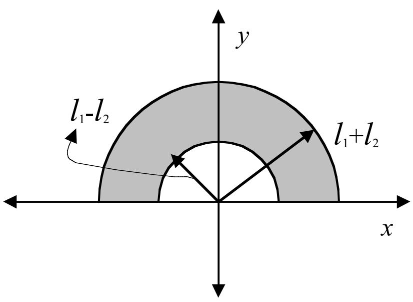

Fig. 2. The workspace of the two link planar manipulator

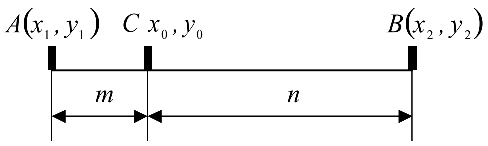

Fig. 3. Dividing the welding seam into step points

of a given step point may calculated. Consider point C in Fig. 3; x_0 and y_0 coordinates are calculated by using geometric equalities as below:

$$\frac{[CA]}{[CB]} = \frac{m}{n} = k \tag{1}$$

then, x_0 and y_0 are written as follow:

$$x_0 = \frac{x_1 + kx_2}{1 + k} \tag{2}$$

and

$$y_0 = \frac{y_1 + ky_2}{1 + k} \tag{3}$$

In Fig. 4 coordinate frames of the two link planar manipulator is given. In this figure, $oxyz$, $ox_1y_1z_1$ and $ox_2y_2z_2$ coordinate frames are placed on the manipulator links according to the Denavit Hartenberger (D-H) representation.[5] The final coordinate system $o_n x_n y_n z_n$ is commonly referred to as the end-effector or tool frame. The origin of the tool frame is most often placed symmetrically between the fingers of the gripper.[6] The unit vectors along the x_n, y_n and z_n axes are labelled as n, s and a, respectively. According to the D-H representation, the transformation matrix in general form can be written as below:

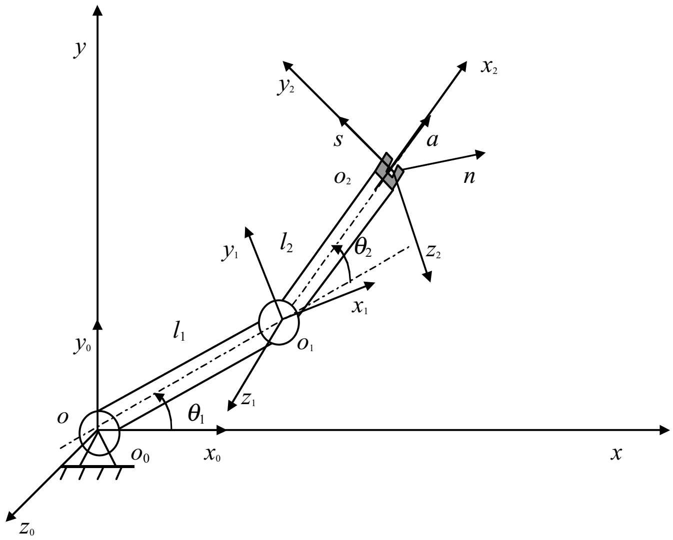

Fig. 4. Coordinate frames attached to two link planar manipulator

$$A_{i-1}^{i} = \begin{bmatrix} Cos\theta_i & -Cos\beta_i Sin\theta_i & Sin\alpha_i Sin\theta_i & a_i Cos\theta_i \\ Sin\theta_i & Cos\alpha_i Sin\theta_i & -Sin\alpha_i Cos\theta_i & a_i Sin\theta_i \\ 0 & Sin\alpha_i & Cos\alpha_i & d_i \\ 0 & 0 & 0 & 1 \end{bmatrix} \tag{4}$$

where $i = 1, 2$. Equation (4) describes the transformation matrix between two coordinate frames i and $(i - 1)$ attached to links i and $i - 1$ which are connected by a rotational joint. In the above equation θ_i is the angle, α_i is the twist angle, a_i is the length and d_i is the distance between the links. The joint variables of the two link planar manipulator are given in Table I.

According to (4), the transformation matrices A_0^1 and A_1^2, which relates to the first and second coordinate frames, can be written as follows:

$$A_0^1 = \begin{bmatrix} c_1 & -s_1 & 0 & l_1c_1 \\ s_1 & c_1 & 0 & l_1s_1 \\ 0 & 0 & 1 & 1 \\ 0 & 0 & 0 & 1 \end{bmatrix}$$
$$A_1^2 = \begin{bmatrix} c_2 & -s_2 & 0 & l_2c_2 \\ s_2 & c_2 & 0 & l_2s_2 \\ 0 & 0 & 1 & 1 \\ 0 & 0 & 0 & 1 \end{bmatrix} \tag{5}$$

Table I. The joints variables.

Link (i)	d_i	a_i	α_i	θ_i
1	0	l_1	0	θ_1
2	0	l_2	0	θ_2

https://doi.org/10.1017/S0263574705002274 Published online by Cambridge University Press

where $c_1 = cos\theta_1$, $s_1 = sin\theta_1$, $c_2 = cos\theta_2$ and $s_2 = sin\theta_2$. The homogeneous transformation matrix is,

$$T = A_0^2 = A_0^1 A_1^2 \tag{6}$$

$$A_0^2 = \begin{bmatrix} c_{12} & -s_{12} & 0 & l_1c_1 + l_2c_{12} \\ s_{12} & c_{12} & 0 & l_1c_1 + l_2c_{12} \\ 0 & 0 & 1 & 1 \\ 0 & 0 & 0 & 1 \end{bmatrix} \tag{7}$$

In the above equation, $c_{12} = c_1c_2 - s_1s_2 = cos(\theta_1 + \theta_2)$ and $s_{12} = s_1c_2 + c_1s_2 = sin(\theta_1 + \theta_2)$. The matrix A_0^2 relates the end-effector coordinates to the base coordinate frame. From Equations (6) and (7), the position of the end-effector in the base coordinate system can be obtained. From (6), A_1^2 can be written as follows:

$$A_1^2 = \left(A_0^1\right)^{-1} T \tag{8}$$

where

$$\left(A_0^1\right)^{-1} = A_1^0 = \begin{bmatrix} c_1 & s_1 & 0 & -l_1 \\ -s_1 & c_1 & 0 & 0 \\ 0 & 0 & 1 & 0 \\ 0 & 0 & 0 & 1 \end{bmatrix},$$

and

$$T = \begin{bmatrix} n_{x0} & s_{x0} & a_{x0} & \bar{P}_{x0} \\ n_{y0} & s_{y0} & a_{y0} & \bar{P}_{y0} \\ n_{z0} & s_{z0} & a_{z0} & \bar{P}_{z0} \\ 0 & 0 & 0 & 1 \end{bmatrix}.$$

Then, Equation (8) can be rewritten as follows

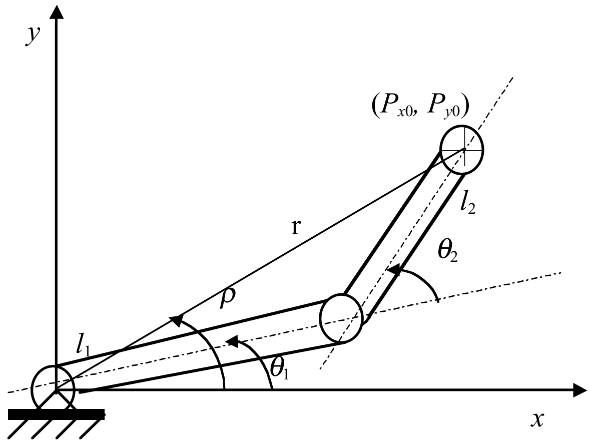

Fig. 5. The manipulator joint angles

where,

$$\begin{aligned} \bar{p}_{x0} &= r\, cos\rho \\ \bar{p}_{y0} &= sin\rho \end{aligned} \tag{13}$$

$$r = \sqrt{\bar{p}_{x0}^2 + \bar{p}_{y0}^2} \tag{14}$$

and $\rho = tan^{-1}(\frac{\bar{p}_{y0}}{\bar{p}_{x0}})$. By using (13) and the equality $cos\theta_1 cos\rho + sin\theta_1 sin\rho = cos(\theta_1 - \rho)$, the Equation (12) is rewritten as below:

$$2l_1 r\, cos(\theta_1 - \rho) = \bar{p}_{x0}^2 + \bar{p}_{y0}^2 + l_1^2 - l_2^2 \tag{15}$$

The above equation can be rewritten by using (14) as;

$$2l_1\sqrt{\bar{p}_{x0}^2 + \bar{p}_{y0}^2}\, cos(\theta_1 - \rho) = \bar{p}_{x0}^2 + \bar{p}_{y0}^2 + l_1^2 - l_2^2 \tag{16}$$

$$A_1^0 T = \begin{bmatrix} c_1 & s_1 & 0 & -l_1 \\ -s_1 & c_1 & 0 & 0 \\ 0 & 0 & 1 & 0 \\ 0 & 0 & 0 & 1 \end{bmatrix} \begin{bmatrix} n_{x0} & s_{x0} & a_{x0} & \bar{P}_{x0} \\ n_{y0} & s_{y0} & a_{y0} & \bar{P}_{y0} \\ n_{z0} & s_{z0} & a_{z0} & \bar{P}_{z0} \\ 0 & 0 & 0 & 1 \end{bmatrix}$$

$$A_1^2 = A_1^0 T \begin{bmatrix} c_1n_{x0} + s_1n_{y0} & c_1s_{x0} + s_1s_{y0} & c_1a_{x0} + s_1a_{y0} & c_1\bar{p}_{x0} + s_1\bar{p}_{y0} - 1_1 \\ -s_1n_{x0} + c_1n_{y0} & s_1s_{x0} + c_1s_{y0} & s_1a_{x0} + c_1a_{y0} & s_1\bar{p}_{x0} + c_1\bar{p}_{y0} \\ n_{z0} & s_{z0} & a_{z0} & \bar{p}_{z0} \\ 0 & 0 & 0 & 1 \end{bmatrix} \tag{9}$$

The corresponding entries in (5) and (9) are set equal, therefore the following equations can be written:

$$c_1\bar{p}_{x0} + s_1\bar{p}_{y0} - l_1 = l_2c_2 \tag{10}$$

$$-s_1\bar{p}_{x0} + c_1\bar{p}_{y0} = l_2s_2 \tag{11}$$

The first and second joint angles, θ_1 and θ_2 in Fig. 5 can be calculated from Equations (10) and (11). Taking the square of (10) and (11) and adding them side by side the following equation results

$$(2l_1\bar{p}_{x0})c_1 + (2l_1\bar{p}_{y0})s_1 = \bar{p}_{x0}^2 + \bar{p}_{y0}^2 + l_1^2 - l_2^2 \tag{12}$$

From (16),

$$cos(\theta_1 - \rho) = \frac{\bar{p}_{x0}^2 + \bar{p}_{y0}^2 + l_1^2 - l_2^2}{2l_1\sqrt{\bar{p}_{x0}^2 + \bar{p}_{y0}^2}} \tag{17}$$

and

$$cos^2(\theta_1 - \rho) = \frac{\left(\bar{p}_{x0}^2 + \bar{p}_{y0}^2 + l_1^2 - l_2^2\right)^2}{4l_1^2\left(\bar{p}_{x0}^2 + \bar{p}_{y0}^2\right)} \tag{18}$$

can be written. By using the equality $cos^2(\theta_1 - \rho) + sin^2(\theta_1 - \rho) = 1$ and Equation (18), the following equation

https://doi.org/10.1017/S0263574705002274 Published online by Cambridge University Press

Table II. The joint variables of the manipulator which are used in the program.

The length of the first link	$l_1 = 10\ cm$
The length of the second link	$l_2 = 9\ cm$
x Coordinate (starting point)	7
y Coordinate (starting point)	5
x Coordinate (ending point)	−7
y Coordinate (ending point)	2
Step Number (n)	50
Total Loggin Time	30 sn

follows

$$sin(\theta_1 - \rho) = \sqrt{1 - \frac{\left(\bar{p}_{x0}^2 + \bar{p}_{y0}^2 + l_1^2 - l_2^2\right)^2}{4l_1^2\left(\bar{p}_{x0}^2 + \bar{p}_{y0}^2\right)}} \qquad (19)$$

From (17) and (19),

$$tan(\theta_1 - \rho) = \frac{\dfrac{\bar{p}_{x0}^2+\bar{p}_{y0}^2+l_1^2-l_2^2}{2l_1\sqrt{\bar{p}_{x0}^2+\bar{p}_{y0}^2}}}{\sqrt{1 - \dfrac{\left(\bar{p}_{x0}^2+\bar{p}_{y0}^2+l_1^2-l_2^2\right)^2}{4l_1^2\left(\bar{p}_{x0}^2+\bar{p}_{y0}^2\right)}}}$$

$$tan(\theta_1 - \rho) = \frac{\sqrt{4l_1^2\left(\bar{p}_{x0}^2 + \bar{p}_{y0}^2\right) - \left(\bar{p}_{x0}^2 + \bar{p}_{y0}^2 + l_1^2 - l_2^2\right)^2}}{\bar{p}_{x0}^2 + \bar{p}_{y0}^2 + l_1^2 - l_2^2} \qquad (20)$$

can be written. Then above equation is;

$$\theta_1 = \rho + tan^{-1}\left[\frac{\sqrt{4l_1^2\left(\bar{p}_{x0}^2 + \bar{p}_{y0}^2\right) - \left(\bar{p}_{x0}^2 + \bar{p}_{y0}^2 + l_1^2 - l_2^2\right)^2}}{\left(\bar{p}_{x0}^2 + \bar{p}_{y0}^2 + l_1^2 - l_2^2\right)}\right] \qquad (21)$$

The second joint angle, θ_2 can be solved by dividing (11) to (10) as below:

$$\theta_2 = tan^{-1}\left(\frac{-\bar{p}_{x0}s_1 + \bar{p}_{y0}c_1}{\bar{p}_{x0}c_1 + \bar{p}_{y0}s_1 - l_1}\right) + k\pi \qquad (22)$$

The program is written acccording to variables which are given in Table II and Equations (21), (22). The algorithm of the program is given in detail in Appendix I.

As it is shown in Table II, the program is run for 30 seconds and 50 step points. After running the program data in Table III are obtained.

IV. RESULTS AND DISCUSSION

The position of the end-effector on the x-axis is shown in Fig. 6. There is a linear relationship between time and position. After the middle of the sampling time (after 15 seconds), the end-effector is moving along the negative part of the x-axis in order to reach to final point set in the program.

Similarly, the variation in the end effector position on the y-axis is shown in Fig. 7. As it is shown in this figure, the starting and ending points of the end-effector matches the values that are given in the program which is rather desirable. It follows from the above two figures the position of the end effector on the xoy coordinate frame is shown in Fig. 8.

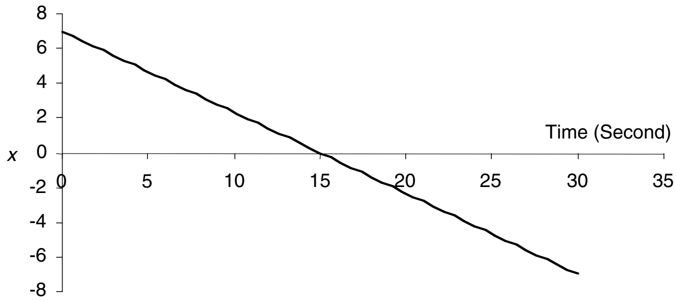

Fig. 6. The position of the end-effector on x-axis

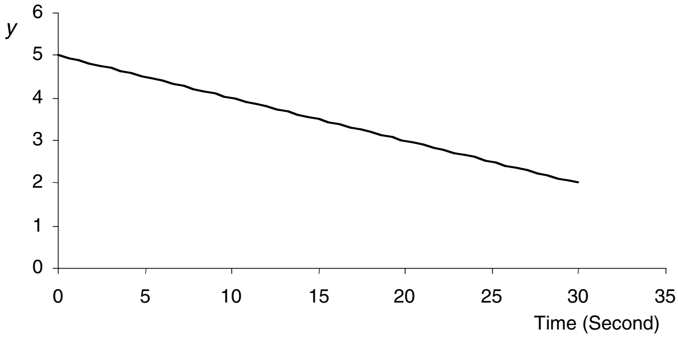

Fig. 7. The position of the end-effector on y-axis

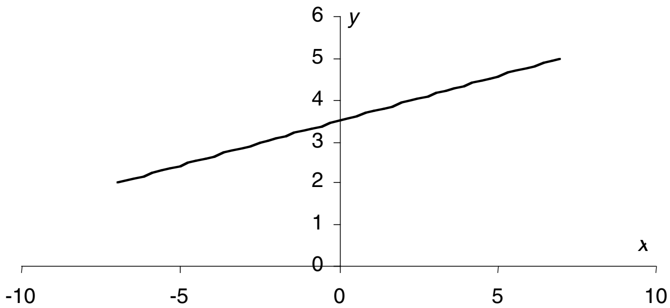

Fig. 8. The position of the end-effector on xoy coordinate frame

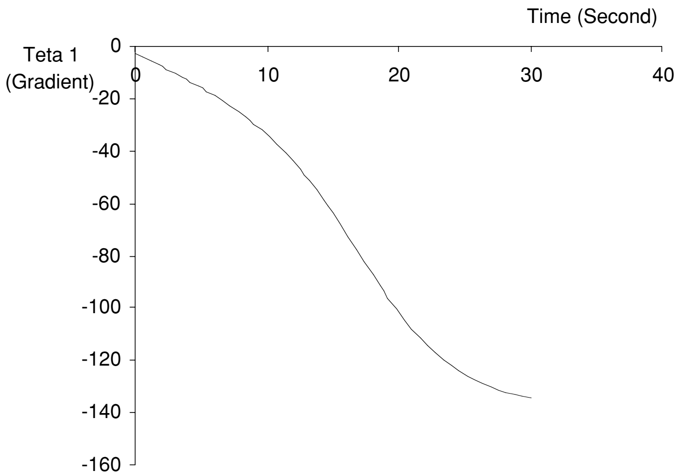

Fig. 9. The variations in the first joint angle, θ_1

The variations in the first joint angle, θ_1 are shown in Fig. 9. In this figure there is a linear relationship between time and the joint angle until 10 sn. After this point, linearity no longer

https://doi.org/10.1017/S0263574705002274 Published online by Cambridge University Press

Table III. The joint variables of the manipulator which are derived from the program.

Step	Time	θ_1 (Gradient)	θ_2 (Gradient)	ω_1 (rad/sn)	ω_2 (rad/sn)
0	0	−2,816486	126,473	0,00	0,00
1	0,6	−4,252487	128,2504	−0,0418	0,0517
2	1,2	−5,715397	130,0042	−0,0426	0,051
3	1,8	−7,208878	131,7343	−0,0434	0,0503
4	2,4	−8,736984	133,4404	−0,0445	0,0496
5	3	−10,30421	135,122	−0,0456	0,0489
6	3,6	−11,91557	136,7784	−0,0469	0,0482
7	4,2	−13,57665	138,4088	−0,0483	0,0474
8	4,8	−15,2937	140,0119	−0,0499	0,0466
9	5,4	−17,07373	141,5863	−0,0518	0,0458
10	6	−18,92464	143,1301	−0,0538	0,0449
11	6,6	−20,85528	144,6412	−0,0562	0,044
12	7,2	−22,8756	146,117	−0,0588	0,0429
13	7,8	−24,99669	147,5543	−0,0617	0,0418
14	8,4	−27,23099	148,9493	−0,065	0,0406
15	9	−29,59219	150,2976	−0,0687	0,0392
16	9,6	−32,09529	151,5941	−0,0728	0,0377
17	10,2	−34,75644	152,8328	−0,0774	0,036
18	10,8	−37,59261	154,0066	−0,0825	0,0341
19	11,4	−40,62097	155,1076	−0,0881	0,032
20	12	−43,85803	156,127	−0,0942	0,0297
21	12,6	−47,31818	157,0547	−0,101	0,027
22	13,2	−51,01178	157,8804	−0,107	0,024
23	13,8	−54,94283	158,593	−0,114	0,0207
24	14,4	−59,10625	159,1815	−0,121	0,0171
25	15	−63,48522	159,6359	−0,127	0,0132
26	15,6	−68,04936	159,9473	−0,133	0,00906
27	16,2	−72,75414	160,1095	−0,137	0,00472
28	16,8	−77,54247	160,1188	−0,139	0,000272
29	17,4	−82,34827	159,9752	−0,14	−0,00418
30	18	−87,10191	159,6816	−0,138	−0,00854
31	18,6	−91,73608	159,2443	−0,135	−0,0127
32	19,2	−96,19121	158,6716	−0,13	−0,0167
33	19,8	−100,4192	157,9736	−0,123	−0,0203
34	20,4	−104,3854	157,1611	−0,115	−0,0236
35	21	−108,0681	156,2452	−0,107	−0,0266
36	21,6	−111,4578	155,2365	−0,0986	−0,0293
37	22,2	−114,5544	154,1449	−0,0901	−0,0318
38	22,8	−117,365	152,9796	−0,0818	−0,0339
39	23,4	−119,9021	151,7484	−0,0738	−0,0358
40	24	−122,1811	150,4586	−0,0663	−0,0375
41	24,6	−124,219	149,1163	−0,0593	−0,039
42	25,2	−126,0335	147,7267	−0,0528	−0,0404
43	25,8	−127,6423	146,2944	−0,0468	−0,0417
44	26,4	−129,0621	144,8232	−0,0413	−0,0428
45	27	−130,3088	143,3162	−0,0363	−0,0438
46	27,6	−131,3971	141,7762	−0,0317	−0,0448
47	28,2	−132,3404	140,2054	−0,0274	−0,0457
48	28,8	−133,1511	138,6058	−0,0236	−0,0465
49	29,4	−133,8403	136,9787	−0,02	−0,0473
50	30	−134,4179	135,3254	−0,0168	−0,0481

exist and the joint angle is varying rapidly. Similar behaviour can be seen in the angular velocity of the first joint angle, as shown in Fig. 10. There, after 1.5 seconds the variations in the joint angle velocity are rapid and nonlinear.

Similarly, the variation in the second joint angle, θ_2 is shown in Fig. 11. In order to reach the required position of the end-effector, the variation in the second joint angle is rather nonlinear, but still there are no sudden increases or decreases, therefore it assumes a gradual form. As a result, the angular velocity of the second joint angle is varying linearly for about 2 seconds, as shown in Fig. 12. After that time the changes are rather nonlinear, but they are still gradual.

https://doi.org/10.1017/S0263574705002274 Published online by Cambridge University Press

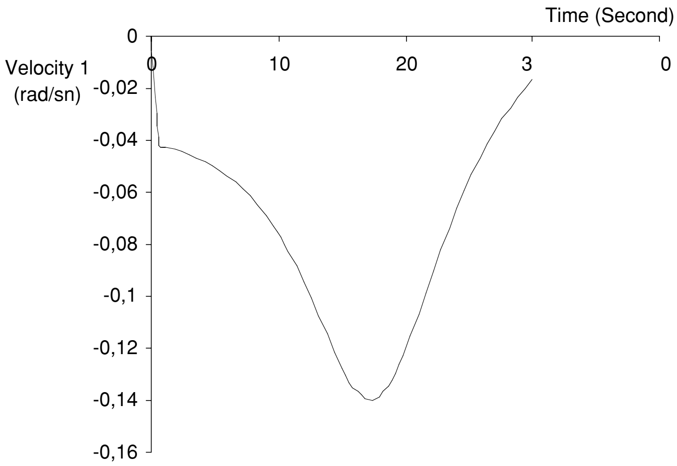

Fig. 10. The changes of the first joint angle velocity, ω_1

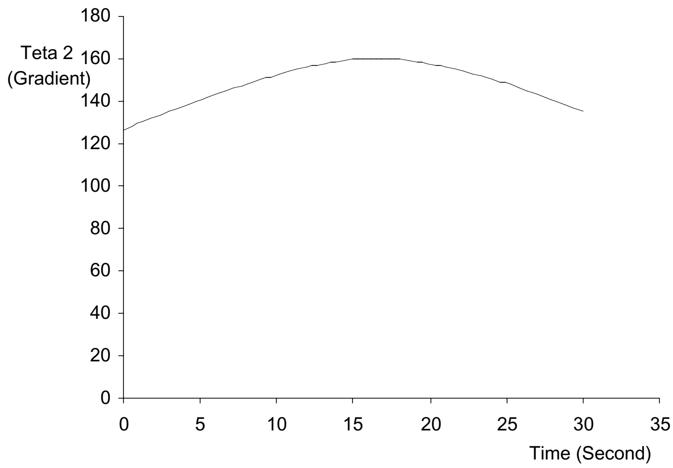

Fig. 11. The variations in the second joint angle, θ_2

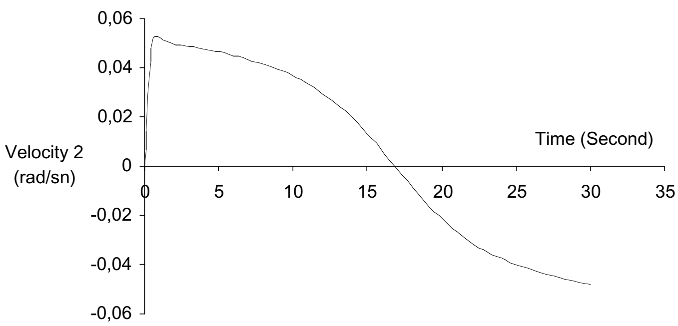

Fig. 12. The changes of the second joint angle velocity, ω_2

V. CONCLUSIONS

In this paper, the joint angles and angular velocities of the two link planar manipulator are derived by using inverse kinematic equations together with some geometric equalities. The joint angles variations and angular velocities are shown in Fig. 6–12. The results derived in this work are completely theoretical.

The program results may give us an idea how the real robot may behave under same condition. Obviously, the real robot may not give same responses. This is due to the fact that in this analyses the mass of the end-effector and links, the friction forces in the joints are not considered.

The variation in the first joint angle, θ_1 is rapid and nonlinear are shown in Fig. 9. This could cause problems, in real life applications due to the fact that under this condition the inertial forces could become very effective; hence, this could lead to instability.

In welding application, the linear movements of the end-effector is crucial in order to have a homogeneous (in terms of materials) welding seam. For that reason, the stability and linear movement of the end-effector is very important. In this case, the stability of the manipulator may be assured by using one of the adaptive control strategies which can adapt itself to changes in the system and working condition.[7]

One could consider modelling the manipulator dynamically by using one of the dynamic system modelling packages program, like *simulink*. The joint angles and position of the links may be found by using this mathematical model of the system. Later on, a prototype of the real manipulator may be built, and the two theoretical results (the inverse kinematic analyses results and the dynamic model results) may be compared with real robot responses in order to see which method is of an effective and practical in use. It is also possible to find which method gives better understanding of the real robot.

References

1. J. C. Colson and N. D. Perreira, "Kinematic Arrangements Used in Industrial Robots", *Proc. 13th International Symposium on Industrial Robots* (1983). pp. 28–37.
2. J. M. Hollerbach and S. Gideon, "Wrist-Partitioned Inverse Kinematic Accelerations and Manipulator Dynamics", *Int. J. Robotics Res.* **4**, 61–76 (1983).
3. A. J. Koivo, *Fundamentals for Control of Robotic Manipulators*, (John Wiley and Sons, 1989).
4. A. A. Goldenberg, B. Benhabib and R. G. Fenton, "A Complete Generalized Solution to the Inverse Kinematics of Robots", *IEEE Journal of Robotics and Automation*, **RA-1**, No. 1, 14–20 (March 1985).
5. M. W. Spong and M. Vidyasagar, *Robot Dynamics and Control* (John Wiley and Sons, 1989).
6. R. P. Paul, B. E. Shimano and G. Mayer, "Kinematic Control Equations for Simple Manipulators" *IEEE Trans. Systems, Man., and Cybernetics* **SMC-11**, No. 6, 339–455 (1981).
7. S. Bulut, "The robustness of Reduced Order Minimal Controller Synthesis Control in Plastic Region", *Proc. Instn Mech. Engrs, Part I, Journal of Systems and Control Engineering* **214**, 185–195 (1999).

APPENDIX I

The calculation program which is written in *Fotran 90*

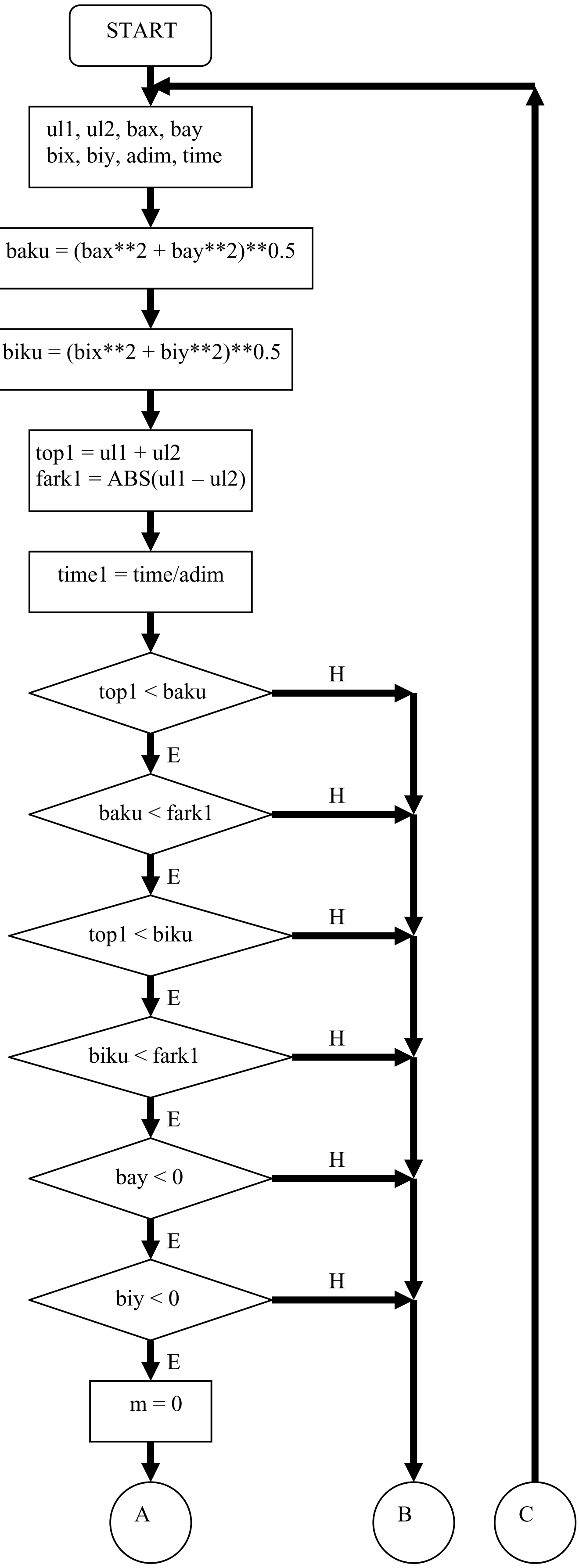

https://doi.org/10.1017/S0263574705002274 Published online by Cambridge University Press

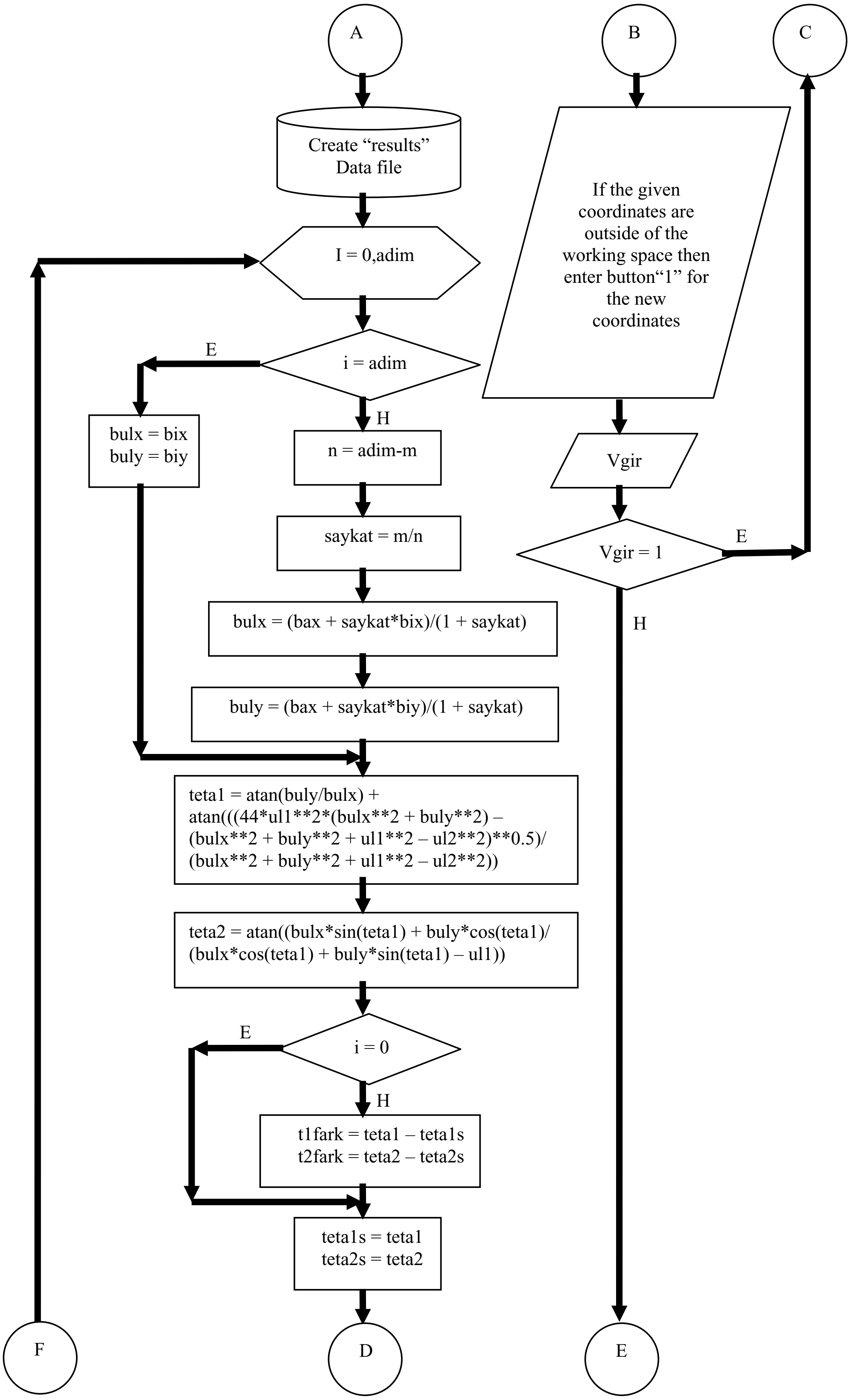

https://doi.org/10.1017/S0263574705002274 Published online by Cambridge University Press

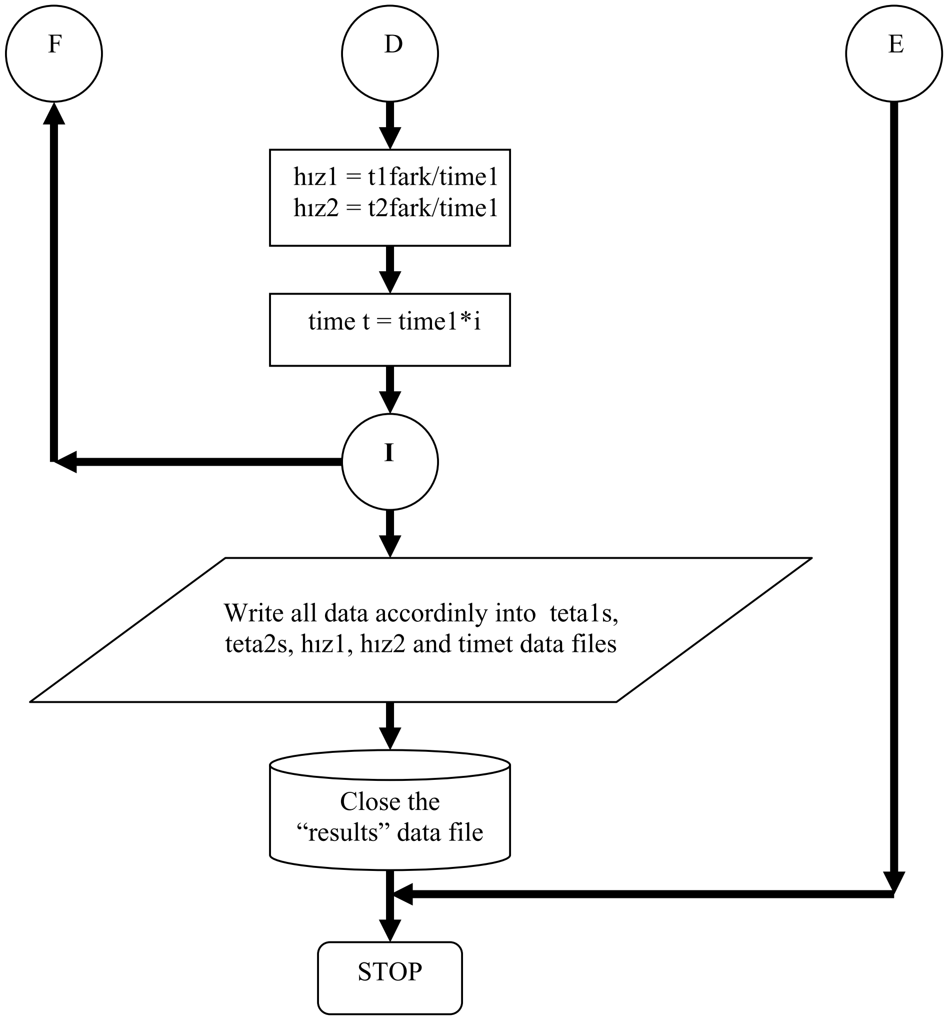

Table IV. The description of notations that are in the Fortran 90 program.

adim: the total step number	n: the total step number along [CB]
baku: the distance between o_0, origin of the base coordinate frame and the starting point	saykat: the coefficient k, $k = m/n$
bax: x coordinate of the starting point	teta1: the first joint angle, θ_1
bay: y coordinate of the starting point	teta2: the second joint angle, θ_2
biku: the distance between o_0, origin of the base coordinate frame and the ending point	teta1s = teta1 − t1fark
	teta2s = teta2 − t2fark
bix: x coordinate of the ending point	t1fark: $\theta_1(t+1) - \theta_1(t)$
biy: y coordinate of the ending point	t2fark: $\theta_2(t+1) - \theta_2(t)$
bulx: x coordinate of the every step point	t: time
buly: y coordinate of the every step point	time: one cycle of time
fark1: the subtractive length of the first and second link	time1: one step of time
	timet: the total time
hız1: the angular velocity of the first joint angle, θ_1	top1: the total length of the first and second link
hız2: the angular velocity of the second joint angle, θ_2	ul1: the length of the first link
m: the total step number along [AC]	ul2: the length of the second link

https://doi.org/10.1017/S0263574705002274 Published online by Cambridge University Press